Experimental and numerical investigations of drop breakage mechanism

Stephanie Hermann[1,*], Sebastian Maaß[1], Daniel Zedel[1], Astrid Walle[2],
Michael Schäfer[2] and Matthias Kraume[1]

[1] Technische Universität Berlin, Chair of Chemical and Process Engineering
Ackerstr. 71-76, 13355 Berlin/Germany
[2] Technische Universität Darmstadt, Institute of Numerical Methods in Mechanical Engineering,
Dolivostr. 15, 64293 Darmstadt/Germany
*E-mail: stephanie.hermann.1@tu-berlin

Abstract
Drop size distributions in turbulent liquid/liquid systems are determined by drop breakage and drop coalescence. In order to describe that distribution mathematically exactly, the physical understanding of each particular process is needed. This work focuses on drop breakage. Single drop breakage events where coalescence can practically be neglected are, therefore, analyzed experimentally by high-speed imaging. The breakage events are induced by a single stirrer blade, part of a Rushton turbine. The influences of the drop diameter (d_p = 0,7 - 3.1 mm), the velocity of the continuous water flow (u_{fluid} = 1.0 - 2.0 m/s) and different dispersed phases (toluene, petroleum, paraffin oils) on the breakage event (breakage probability, location and time) are investigated. To determine and describe the breakage mechanism, the experimental results are correlated with the flow properties of the continuous phase, gained by Computational Fluid Dynamics. The regions with the highest energy dissipation rates and the velocity field are compared with the experimental results - especially the drop breakage location. For the system petroleum/water (d_p = 1.0 mm) drop breakage can be explained by the microstructure of turbulence. The turbulent fluctuations lead to drop breakage. With increasing droplet stability (resulting from physical properties) or increasing droplet diameters, the macrostructure of turbulence has to be considered to explain drop breakage exactly. Gradients of the mean velocities in the vortices behind the stirrer blade contribute to drop breakage.

Keywords: drop breakage mechanism, modeling, liquid/liquid systems, Rushton turbine, Computational Fluid Dynamics

1. Introduction

There are numerous applications in industry, where reactions and mass, as well as energy transfer between two immiscible fluids are the major concerns. When trying to influence or predict the contact area one has to focus on drop sizes and the underlying principles that lead to the formation of drops in immiscible liquid/liquid dispersions, for example in stirred tanks.

The drop formation and the resulting drop size distributions are determined by drop breakage and coalescence. In order to predict drop size distributions, both phenomena have to be understood and described mathematically exactly.

Comprehensive scientific research identified a multitude of theoretical models describing both processes, recently summarized by Liao and Lucas (2009/2010). Nevertheless, the prediction of drop size distributions, when varying power input, material and process parameters, is only possible with restrictions. Consequently, the models for breakage and coalescence need further improvement.

Drop breakage occurs, when the external forces and stresses, exerted on particles by the continuous phase, exceed the internal forces and stresses, which keep the particle together (Hinze, 1955; Liao and Lucas, 2009 and others).

It is widely accepted to describe the maximum stable drop diameter and, therefore, drop breakage, by means of considering the dynamic pressure forces of the turbulent motions, applying Kolmogoroffs´s theory of turbulence. These dynamic pressure forces are caused by changes in velocity around the particle. As the turbulent velocity fluctuations are a function of the local energy dissipation rate (Hinze, 1955; Shinnar and Church, 1960), it can be used to describe drop breakage.

Kumar *et al.* (1991) stated that besides the turbulent fluctuations other breakage mechanisms occur. Therefore, they suggested that the shear layer on the blade and the elongation flow along the impeller length also influence drop breakage.

Liao and Lucas (2009) distinguish between four mechanisms that can influence fluid particle

breakup, namely turbulent fluctuation, viscous shear forces, shearing-off process and interfacial instability.

To investigate drop breakage experimentally, single drop breakage examinations, where coalescence can be neglected, have been widely used. Thereby, number and/or size distributions of broken droplets, breakage probabilities, times and/or deformations are determined experimentally. This allows a validation and improvement of drop breakage modeling and a deeper understanding of the occurring mechanism that leads to drop breakage, accordingly. An overview of such investigations can be found in Maaß and Kraume (2011) and Maaß *et al.* (2011). Besides, there is literature available addressed to breakage modeling, that includes experimental investigations of drop breakage, coupled with the local flow properties or rather flow stress.

For instance, Galinat *et al.* (2007a/b) investigated drop breakage in a pipe, downstream of an orifice, considering the local flow properties, which were gained by PIV measurements.

Furthermore, Maniero *et al.* (2010) conducted Direct Numerical Simulation of that pipe and coupled the resulting velocity field to a Lagrangian tracking of individual particles. They compared calculated locations of breakup events to experimental results. Detailed information on the external stresses experienced by the drops, can be achieved by these simulations.

Aim of this work is to determine breakage mechanisms, depending on size and physical properties of the droplets. Hence, experimentally determined drop breakage behaviour (breakage probability, time and location) is compared with fluid flow characteristics in stirred systems.

The method used to analyze drop breakage is to investigate single drop breakage events. The experiments were carried out in a special breakage channel (Maaß *et al.*, 2007/2009), described below. It simplifies the flow field in a stirred tank and simulates the region around the impeller. Maaß *et al.* (2009) proved this simplification by experimental and numerical investigations, comparing the fluid conditions in a stirred tank with those in the drop breakage cell.

Since CFD has become a standard tool for flow prediction (see for instance Joshi *et al.*, 2011), the single-phase simulation is an advantageous opportunity to yield reliable information about the flow and is used here, to determine the flow properties of the continuous water phase.

2. Experimental and numerical set up

2.1 Experimental set up

The experimental set up used, is depicted in Fig. 1. A single blade of a Rushton turbine (d = 0.08 m) is mounted in a rectangular channel (30 mm x 30 mm). Drop breakage in the vicinity of the stirrer blade is investigated by high-speed imaging.

Drops (d_p = 0.7-3.1 mm) are generated with a Hamilton® dosing pump PSD/3 in the lower part of the channel (see Fig. 1).

In order to get statistically significant results, at least 1000 sequences of droplets entering the area of interest, are recorded for one parameter set (constant flow velocity, droplet phase and diameter). Pictures are taken with 822 frames per second.

The breakage events are analyzed by automated image recognition described by Maaß *et al.* (2007) and Maaß and Kraume (2011).

In this work, the number of breaking drops is set into relation to the total number of investigated droplet sequences, to calculate the breakage probability P.

The breakage time $t_{b,\beta}$ is defined to be the interval between the time when the drop passes the stirrer blade and the time when breakage occurs, that means, more than one drop is visible on the picture. It is determined by dividing the frame number by the frame rate. Thereby, not the averaged mean value, but the maximum of an adapted β-distribution is used to characterize the breakage time. For a more detailed explanation see Maaß and Kraume (2011).

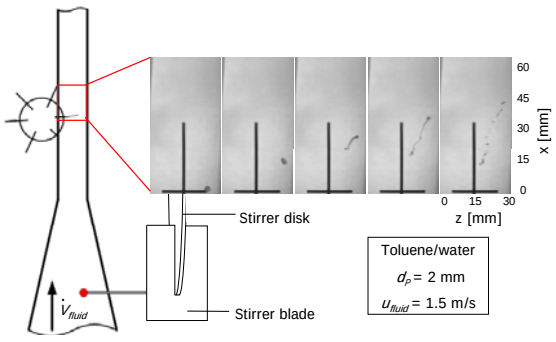

Fig. 1 Experimental set up and drop breakage for a toluene droplet (d_p = 2.0 mm, u_{fluid} = 1.5 m/s, Δt = 5 ms).

Pictures are taken with 286 x 608 pixel and a resolution of about 10 pixel/mm. The breakage location is calculated by averaging the x- and y-location of the centres of gravity of all the daughter drops after first breakage. The region of interest

(beginning at the stirrer blade) is divided into squares with a side length of 26 pixel and the relative breakage probability in each square is shown in a 2-dimensional contour plot. It is defined as the ratio of the number of droplets breaking in one square to the total number of broken droplets for the investigated parameter set.

Table 1 Physical properties of the investigated droplet substances.

	$\gamma_{with\ dye}$ [mN/m]	ρ_d [kg/m^3]	η_d [mPas]
Toluene	32	870	0.55
Petroleum	38.5	790	0.65
Paraffin oil 10	42	807	8
Paraffin oil 100	62	850	125

Four different dispersed phases were used for the investigations. All were blended with a non-water soluble dye (c = 0.075 g/L) to increase the optical properties of the image data. The physical properties of the investigated systems are listed in table 1.

The velocity of the continuous flow was varied between u_{fluid} = 1.0 and 2.0 m/s, which corresponds to typical relative velocities between the stirrer and the fluid flow in a stirred tank.

2.2 Numerical set up

The numerical simulations of the flow in the channel are performed with the in-house flow solver FASTEST-3D.

For the considered flow velocities at the stirrer blade of u_{fluid} = 1.0, 1.5 and 2.0 m/s, the flow in the breakage channel around the blade has high Reynolds-numbers (Re ≈ 20000-30000) and is consequently turbulent. The turbulence is taken into account by performing steady RANS simulations with the standard high-Re k- ε model. Using this 2-equation model from Launder and Spalding, the turbulent fluctuations are averaged and the resulting term for the Reynolds stresses is modeled with the Boussinesq-hypothesis. The flow region is spatially discretized with a blockstructured grid with 1000000 control volumes (y^+ ≈ 20-70).

To ensure a realistic inlet profile for the velocity and the turbulent quantities k and ε, an additional periodic channel is simulated (see Fig. 2). During the simulation of the flow in the breakage channel, the flow through the periodic channel is simultaneously calculated. In every iteration a plane from the periodic channel is copied to the inlet of the breakage channel.

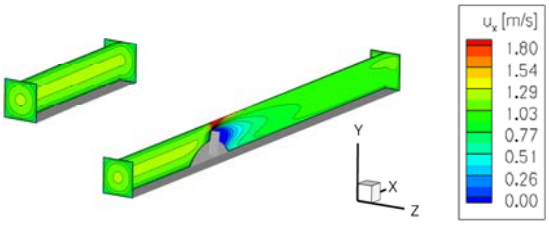

Fig. 2 Numerical set up: periodic channel (3 Mio elements – left side) and drop breakage channel (8 Mio elements – right side) for a fluid flow velocity of u_{fluid} = 1.5 m/s.

3. Results and Discussion

3.1 Influence of the fluid flow velocity

Experimentally determined drop breakage locations for a toluene droplet and a fluid flow velocity of u_{fluid} = 1.5 m/s are depicted in Fig. 3. On the left side, each single breakage event is projected on a 2-dimensional grid of the investigated region. In the middle, the same data is plotted as a contour plot and on the right side of the figure, the relative breakage probability is shown from another point of view. Considering both views, it becomes evident, that droplets are breaking most frequently directly after the stirrer. With increasing distance from the stirrer blade, the drop breakage probability decreases, which corresponds well with the local energy dissipation rates (see Fig. 4). The highest energy dissipation rates are located directly at the three free edges of the stirrer blade and behind; it decreases with increasing distance from the stirrer blade.

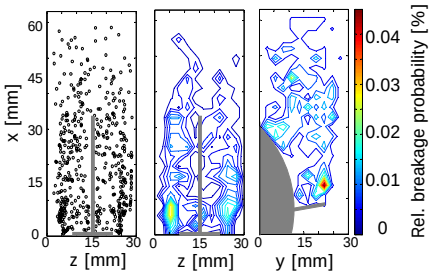

Fig. 3 Experimentally determined breakage locations for a toluene droplet (d_p = 1.0 mm, u_{fluid} = 1.5 m/s).

In Fig. 3 it becomes evident, that more droplets break on the left and on the right side of the stirrer blade, than in the centre of the channel. Maaß *et al.* (2009) investigated the entrance distribution of the

droplets for several set ups. They found out, that much more droplets are entering the analyzed area from the right and the left of the stirrer blade, than in the centre of the channel, which corresponds to the occurring breakage events.

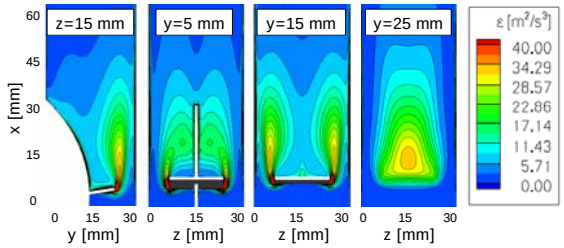

Fig. 4 Calculated energy dissipation rates in the drop breakage channel for a fluid flow velocity at the stirrer blade of u_{fluid} = 1.5 m/s.

Increasing the fluid flow velocity corresponds to higher stirrer speeds in stirred tanks and therefore greater power inputs. For this investigation, the fluid flow velocity was varied between u_{fluid} = 1.0 and 2.0 m/s. Petroleum was used as the droplet phase (d_p = 1.0 mm). In Fig. 5 a comparison between the experimentally determined drop breakage location (left side) and the calculated local energy dissipation rates (right side) is presented. As Maaß *et al.* (2009) already showed experimentally for a toluene/water system (d_p = 1.0 mm), at low velocities drop breakage occurs only in the region behind the stirrer blade, where the energy dissipation, or rather the turbulent fluctuations, are big enough to break droplets. Drop breakage terminates much earlier behind the blade for this lower fluid flow velocity. For the higher one, where high energy dissipation rates are localized at a greater distance from the blade, droplets can still be broken in that area behind the blade.

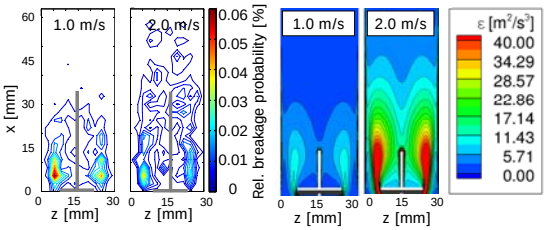

Fig. 5 Experimentally determined relative breakage probabilities in comparison to calculated energy dissipation rates at y=10 mm for fluid flow velocities at the stirrer blade of u_{fluid}=1.0 and 2.0 m/s (petroleum, d_p = 1.0 mm).

Due to higher power input when increasing the fluid flow velocity, the breakage probability increases from P = 53 (u_{fluid}=1.0 m/s) to 75 % (u_{fluid} = 2.0 m/s), while the breakage time decreases from $t_{b,\beta}$ = 4.4 to 2.8 ms.

3.2 Influence of the system properties

To discuss the influence of the system properties, three different substances, namely toluene, the low viscosity paraffin oil 10 and the high viscosity paraffin oil 100, are compared (for the physical properties see table 1). The particle diameter (d_p = 1.0 mm) and the fluid flow velocity (u_{fluid} = 1.5 m/s) were kept constant.

The more stable the droplets are (increasing viscosities and interfacial tensions), the less breakage events far away from the stirrer blade could be recorded and the earlier behind the stirrer blade drop breakage ends (see Fig. 6, stability increases from left to right). Only toluene, with the lowest viscosity and interfacial tension, can be broken far behind the stirrer blade, almost at the end of the investigated region.

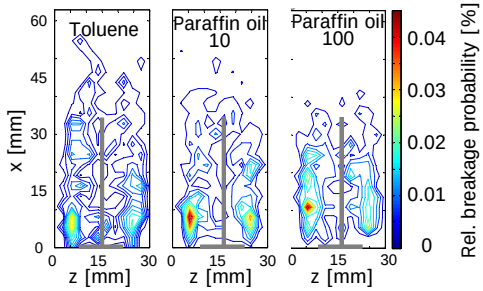

Fig. 6 Experimentally determined influence of the droplet substance on relative breakage probabilities (d_p = 1.0 mm, u_{fluid} = 1.5 m/s).

Additionally, the regions of greater relative breakage probabilities get stretched and move away from the stirrer blade with increasing stability of the droplets. This can be clearly seen for the high-viscosity paraffin oil 100, where the breakage events did not take place as close to the blade as for the other substances. In that case, drop breakage is not concentrated in the region of the highest energy dissipation rate.

The breakage probability decreases with increasing droplet stability (see table 2). The high viscosity paraffin oil 100 has by far the lowest breakage probability. Furthermore, the breakage time is significantly increased for the high viscosity paraffin oil. That could be one explanation for the outstanding breakage location distributions of the high viscosity paraffin oil 100/water system. When deformation starts in the regions with high energy dissipation rates, breakage finally occurs at a greater

distance from the stirrer blade, than for any of the other systems. Breakage initiation correlates with the maximum local energy dissipation rates.

Table 2 Breakage probability P and breakage time $t_{b,\beta}$ for the three investigated systems (d_p = 1.0 mm, u_{fluid} = 1.5 m/s).

	P [%]	$t_{b,\beta}$ [ms]
Toluene/water (Maaß and Kraume, 2011)	60	3.4
Paraffin oil 10/ water	58	3.8
Paraffin oil 100/ water	26	8.5

Considering the mean flow velocities and the resulting flow field (see Fig. 7) it becomes evident, that especially the drop breakage of the high viscosity paraffin oil can be explained by the macrostructure of turbulence.

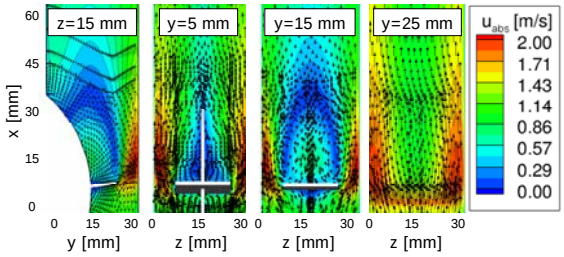

Fig. 7 Velocity field in the drop breakage channel for a fluid flow velocity at the stirrer blade of u_{fluid} = 1.5 m/s.

Drop breakage occurs in the region where the vortices behind the stirrer blade are located (see Fig. 7 at y=15 mm) and, therefore, gradients of the mean velocities are existent. According to Stoots and Calabrese (1995), the breakage cell represents a rotating frame of reference. That flow is characterized by a wake behind the stirrer blade, which consists of two vortices (Maaß *et al.,* 2009). Additionally, it can be seen that the flow at the edges of the stirrer blade is considerably accelerated, which leads to deformation, or rather elongation, of the particles when arriving at the tip region and also contributes to the breakage process.

3.3 Influence of droplet diameter

The smallest and thus most stable droplet has a distinct maximum close to the stirrer blade, where most of the droplets break (see Fig. 8). When increasing the droplet diameter, this area gets wider; the droplets break more homogenously over the investigated area. As Maaß *et al.* (2009), who investigated two droplet diameters of a toluene/water system, already pointed out, this can be explained by the surface forces of the drop. The smaller droplet is more stable than the larger one and so breakage occurs in the region with the highest energy dissipation rates, close to the stirrer blade. With increasing droplet diameter the region were droplets break is extended further behind the stirrer blade.

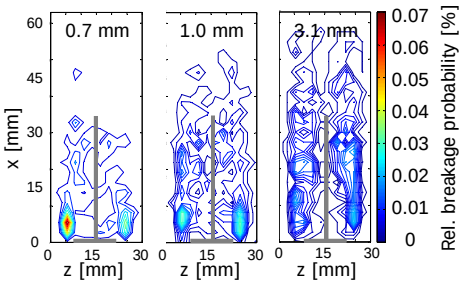

Fig. 8 Experimentally determined influence of the droplet diameter on relative breakage probabilities (petroleum, u_{fluid} = 1.5 m/s).

That goes along with increasing breakage probabilities and increasing breakage times (P = 50%, $t_{b,\beta}$ = 3.4 ms for d_p = 0.7 mm, P = 82%, $t_{b,\beta}$ = 13.3 for d_p = 3.1 mm) (Maaß *et al.*, 2011).

For the biggest investigated droplet (d_p = 3.1 mm), the region with the maximum of breaking droplets does not start directly behind the stirrer blade. That again can be explained by the increased breakage time, which leads to considerable deformation after entering the investigated area before breakage. Furthermore, from that experimentally determined breakage probability distribution, it can be concluded, that not only the microstructure of turbulence, but again also the macro vortices behind the stirrer blade contribute to the drop breakage.

4. Conclusions

In this work single drop breakage events were analyzed experimentally by high-speed imaging. The influence of the droplet substance and diameter, as well as the influence of the flow velocity on drop breakage, were determined. The experimental results were compared with the fluid flow properties, gained by CFD, to get a deeper understanding of the drop breakage mechanism.

Experimentally determined drop breakage locations correlate well with the local energy dissipation rates for a petroleum/water system (d_p = 1.0 mm). Drop breakage can be explained by

the microstructure of turbulence, which means that turbulent fluctuations lead to drop breakage.

In contrast, when increasing the droplet stability significantly (different physical properties), not only the microstructure of turbulence should be used to describe the drop breakage process exactly, but also the macrostructure has to be considered. As a big amount of droplets break in the region behind the stirrer blade where the vortices are located, gradients of the mean velocity contribute to the breakage process. The same was found when increasing the droplet diameter.

Acknowledgment

The authors acknowledge the German Research Foundation (Deutsche Forschungsgemeinschaft – DFG) for their financial support within the project „Modelling, Simulation, and Control of Drop Size Distributions in Stirred Liquid/liquid Systems“.

Nomenclature

c	=concentration (g/L)
d	=stirrer diameter (m)
d_p	=particle or droplet diameter (m)
k	=turbulent kinetic energy (m^2/s^2)
t	=time (s)
$t_{b,\beta}$	=breakage time (s)
u_{fluid}	=velocity of the continuous flow (m/s)
u_x	=velocity in x-direction (m/s)
P	=Breakage probability [%]
Re	=Reynolds number [-]
$y+$	=dimensionless wall distance [-]
Greek letters	
γ	=interfacial tension (mN/m)
ε	=energy dissipation rate (m^2/s^3)
η_d	=dynamic viscosity of the droplet phase (mPas)
ρ_d	=density of the droplet phase (kg/m^3)

Literature Cited

Galinat, S., Risso, F., Masbernat, O., Guiraud, P. Dynmics of drop breakup in inhomogeneous turbulence at various volume fractions. *J. Fluid Mech.*, 578, 85-94 (2007a).

Galinat, S., Torres, L.G., Masbernat, O., Guiraud, P., Risso, F., Dalmazzone, C., Noik, C. Breakup of a drop in a liquid-liquid pipe flow through an orifice. *AIChE,* 53, 56-68 (2007b).

Hinze, J. O. Fundamentals of the Hydrodynamic Mechanism of Splitting in Dispersion Processes. *AIChE*, 1, 289-295 (1955).

Joshi, J.B., Nere, N.K., Rane, C.V., Murthy, B.N., Mathpati, C.S., Patwardhan, A.W., Ranade, V.V. CFD Simulation of Stirred Tanks: Comparison of Turbulence Models. Part I: Radial Flow Impellers. *Can. J. Chem. Eng.*, 89, 23-82 (2011).

Kumar, S., Kumar, R., Gandhi, K.S. Alternative Mechanisms of Drop Breakage in Stirred Vessels. *Chem. Eng. Sci.*, 46, 2483-2489 (1991).

Liao, Y., Lucas, D. A literature review of theoretical models for drop and bubble breakup in turbulent dispersions. *Chem. Eng. Sci.,* 62, 3389-3406 (2009).

Liao, Y. X., Lucas, D. A literature review on mechanisms and models for the coalescence process of fluid particles. *Chem. Eng. Sci.,* 65, 2851-2864 (2010).

Maaß, S., Buscher, S., Hermann, S., Kraume, M. Analysis of particle strain in stirred bioreactors by drop breakage investigations. *Biotech. J.*, accepted, DOI: 10.1002/biot.201100161 (2011).

Maaß, S., Gäbler, A., Zaccone, A., Paschedag, A.R., Kraume, M. Experimental investigations and modelling of breakage phenomena in stirred liquid/liquid systems. *Chem. Eng. Res. Des.*, 85, 703-709 (2007).

Maaß, S., Kraume, M. Determination of breakage rates with single drop experiments. *Chem. Eng. Sci.,* submitted (2011).

Maaß, S., Wollny, S., Sperling, R., Kraume, M. Numerical and experimental analysis of particle strain and breakage in turbulent dispersions. *Chem. Eng. Res. Des.,* 87,565-572 (2009).

Maniero, R., Masbernat, O., Climent, E., Roisso, F. Modelling and simulation of drop break-up downstream of an orifice. *7th International Conference on Multiphase Flow*, Tampa, Florida, USA (2010).

Shinnar, R. Church, J.M. Statistical Theories of Turbulence in ... Predicting Particle Size in Agitated Dispersions. *Ind. Eng. Chem.,* 52, 253-256 (1960).

Stoots, C. M., Calabrese, R.V. Mean Velocity-Field Relative to a Rushton Turbine Blade. *AIChE*, 41, 1-11 (1995).